Developmental Biology xxx (xxxx) xxx

Contents lists available at ScienceDirect

Developmental Biology

journal homepage: www.elsevier.com/locate/developmentalbiology

Short Communication

Left-right asymmetric heart jogging increases the robustness of dextral heart looping in zebrafish

Daniel T. Grimes [a,b], Victoria L. Patterson [a], Gabriel Luna-Arvizu [b], Jodi Schottenfeld-Roames [a], Zoe H. Irons [b], Rebecca D. Burdine [a,*]

[a] Molecular Biology Department, Princeton University, Princeton, NJ, United States
[b] Institute of Molecular Biology, Department of Biology, University of Oregon, Eugene, OR, United States

ARTICLE INFO

Keywords:
Left-right asymmetry
Chirality
Zebrafish
Heart looping
Morphogenesis
Heterotaxy
Nodal
Heart jogging

ABSTRACT

Building a left-right (L-R) asymmetric organ requires asymmetric information. This comes from various sources, including asymmetries in embryo-scale genetic cascades (including the left-sided Nodal cascade), organ-intrinsic mechanical forces, and cell-level chirality, but the relative influence of these sources and how they collaborate to drive asymmetric morphogenesis is not understood. During zebrafish heart development, the linear heart tube extends to the left of the midline in a process known as jogging. The jogged heart then undergoes dextral (i.e. rightward) looping to correctly position the heart chambers relative to one another. Left lateralized jogging is governed by the left-sided expression of Nodal in mesoderm tissue, while looping laterality is mainly controlled by heart-intrinsic cell-level asymmetries in the actomyosin cytoskeleton. The purpose of lateralized jogging is not known. Moreover, after jogging, the heart tube returns to an almost midline position and so it is not clear whether or how jogging may impact the dextral loop. Here, we characterize a novel loss-of-function mutant in the zebrafish Nodal homolog *southpaw* (*spaw*) that appears to be a true null. We then assess the relationship between jogging and looping laterality in embryos lacking asymmetric Spaw signals. We found that the probability of a dextral loop occurring, does not depend on asymmetric Spaw signals per se, but does depend on the laterality of jogging. Thus, we conclude that the role of leftward jogging is to spatially position the heart tube in a manner that promotes robust dextral looping. When jogging laterality is abnormal, the robustness of dextral looping decreases. This establishes a cooperation between embryo-scale Nodal-dependent L-R asymmetries and organ-intrinsic cellular chirality in the control of asymmetric heart morphogenesis and shows that the transient laterality of the early heart tube has consequences for later heart morphogenetic events.

1. Introduction

Asymmetry recurs across scales in development. On a large scale, the internal structure of many animals is highly asymmetric between the left and right sides. In vertebrate embryos, Nodal signaling is activated in the left lateral plate mesoderm (LPM) but remains inactive in the right LPM; this embryo-scale left-right (L-R) asymmetry presages and dictates the lateralization of many organs (Grimes and Burdine, 2017). At a smaller scale, individual cells can possess inherent chirality owing to cytoskeletal and other asymmetries (Bornens, 2012; Wan et al., 2016). This chirality can influence organ-level asymmetries during morphogenesis (Lebreton et al., 2018; Ray et al., 2018; Taniguchi et al., 2011; Tee et al., 2015), but how these asymmetries impinge upon one another and are integrated across scales during embryogenesis is little-understood (Grimes, 2019; Levin et al., 2016).

The zebrafish heart is positioned to the left, as in mammals, and is patterned in a L-R asymmetric fashion (Fig. 1A). Initially, cardiac precursor cells migrate from lateral positions and fuse at the midline to form a symmetrical cardiac cone (Grant et al., 2017; Holtzman et al., 2007). Asymmetry then emerges in stages. The cone rotates and telescopes into a tube with the venous end pointing toward the left, a process termed cardiac jogging (Chen et al., 1997; Stainier et al., 1993). The laterality of jogging is controlled by embryo-scale L-R asymmetries in the Nodal pathway (Baker et al., 2008; de Campos-Baptista et al., 2008; Rohr et al., 2008). Specifically, the zebrafish Nodal homolog Southpaw (Spaw), which is expressed in the left lateral plate mesoderm (LPM), signals to the left side of the heart cone and there increases the velocity of myocardial cell migration; posterior cells migrate to the anterior-left, causing

* Corresponding author.
E-mail address: rburdine@princeton.edu (R.D. Burdine).

https://doi.org/10.1016/j.ydbio.2019.11.012
Received 17 April 2019; Received in revised form 18 November 2019; Accepted 19 November 2019
Available online xxxx
0012-1606/

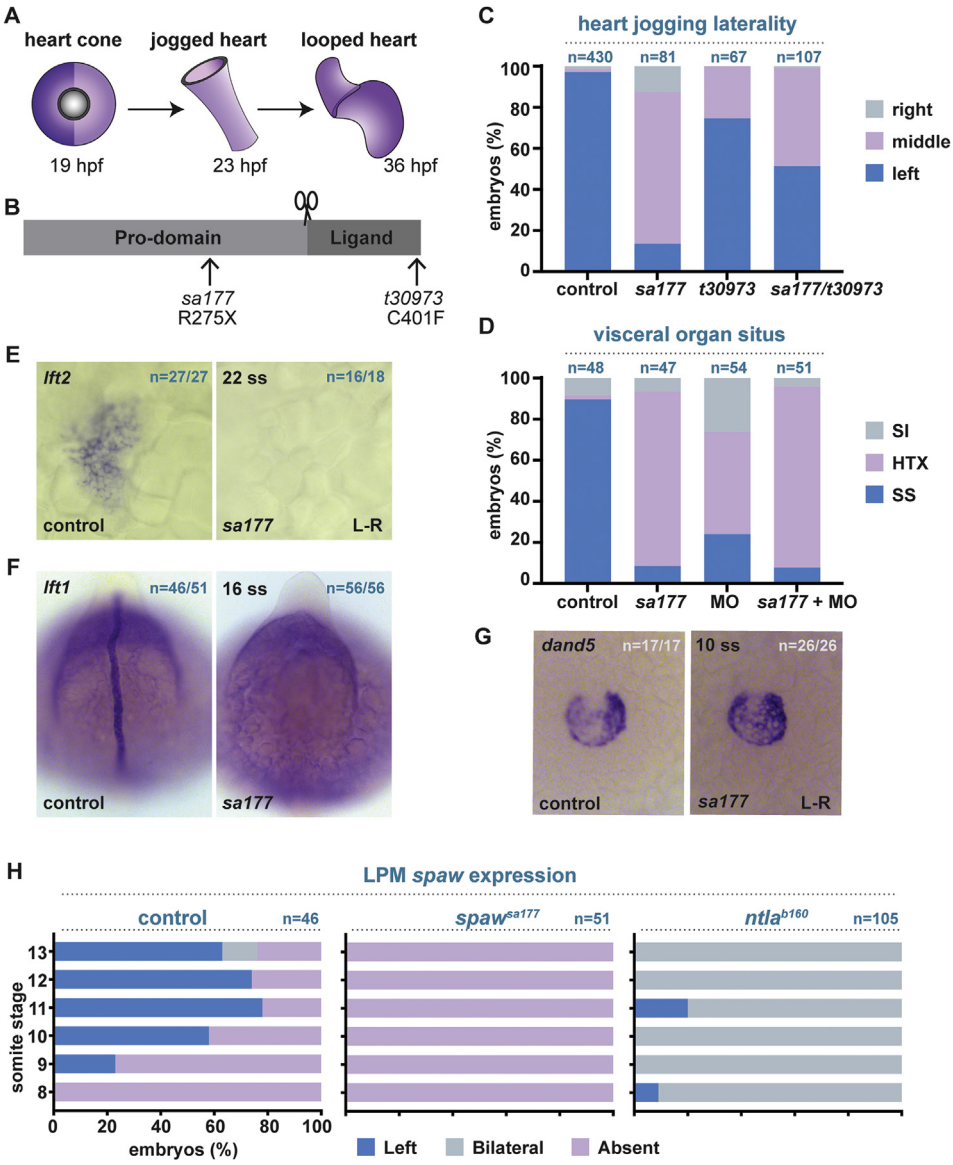

Fig. 1. Abnormal organ asymmetry and loss of Spaw target genes in *spaw*^{sa177} mutants. (**A**) Schematic of heart stages studied in this manuscript. The heart initially forms a symmetrical cone at 19 hpf; Spaw signaling activates *lft2* expression in the left side of the cone (dark purple; dorsal view). Shortly after, by 23 hpf, the heart has formed a tube which is positioned to the left side (dorsal view). By 36 hpf, the heart has undergone looping morphogenesis to produce a dextrally looped heart (*en face* view). (**B**) The Spaw protein consists of a pro-domain and signaling ligand domain that are separated by proteolytic cleavage. The positions of the *spaw*^{sa177} mutation (R275X) and *spaw*^{t30973} mutation (C401F) are shown. (**C**) Jogging direction in control, *spaw*^{sa177}, *spaw*^{t3097} and *spaw*$^{sa177/t30973}$ mutants, assessed by *myl7* ISH at 23 hpf. All samples were statistically significantly different from each other ($p < 0.05$; chi-square test) (**D**) Visceral organ situs in control, *spaw*^{sa177}, *MO*^{spaw} and *spaw*^{sa177};*MO*^{spaw} embryos, assessed by ISH at 48 hpf for heart, liver and pancreas. All samples were statistically significantly different from each other ($p < 0.05$) except *spaw*^{sa177} and *spaw*^{sa177};*MO*^{spaw} ($p > 0.05$; chi-square test). (**E-G**) Expression of *lft2* (E), *lft1* (F) and *dand5* (G) in control and *spaw*^{sa177} mutants at the indicated somite stages (ss). (**H**) Lateral plate mesoderm (LPM) *spaw* expression was scored by ISH across a range of ss for *spaw*^{sa177} and *ntla*^{b160} mutants. hpf – hours post fertilization; ss – somite stage; SS – *situs solitus*; HTX – heterotaxy; SI – *situs inversus*.

rotation and leftward movements of the cone (Baker et al., 2008; de Campos-Baptista et al., 2008; Lenhart et al., 2013; Rohr et al., 2008; Smith et al., 2008). Mathematical modeling suggests that these L-R differential migration velocities are sufficient to generate leftward-pointing heart tubes (Veerkamp et al., 2013). Despite this progress in understanding the mechanisms of leftward jogging, it remains unclear what functional role jogging plays in heart morphogenesis: tubes point leftward from 23 to 28 h post fertilization (hpf), but are ultimately repositioned near to the midline (Chin et al., 2000).

Jogging is followed by heart looping, where, from 30 hpf, the tube bends rightwards to produce a dextral S-shaped heart with the ventricle to the right of the atrium (Desgrange et al., 2018; Grant et al., 2017). Looping laterality may be influenced by embryo-scale asymmetries; defects in the Spaw pathway can generate abnormally lateralized heart loops including mirror-imaged sinistral loops as well as hearts that fail to loop in a lateralized manner and instead retain a middle position where the atrium and ventricle are both positioned along the midline (Baker et al., 2008; Montague et al., 2018). However, hearts cultured *ex vivo* still loop dextrally in the majority of cases, suggesting that looping laterality is mostly controlled by heart-intrinsic asymmetries rather than embryo-scale Spaw asymmetry (Noel et al., 2013).

Here, we present a new *spaw* loss-of-function mutation (*spaw*^{sa177}) in zebrafish which exhibits phenotypic differences to previously reported *spaw* models. We find that *spaw*^{sa177} mutants lack Spaw target gene expression, suggesting that it is a null. We then use *spaw*^{sa177} to understand how left-lateralized jogging and dextral looping are impacted by loss of the Spaw asymmetric pathway. We demonstrate that the heart-intrinsic mechanism of generating dextral loops is modified by jogging direction in a Spaw-independent fashion. This suggests that the hitherto unknown role of jogging in zebrafish is to position the heart tube in order to promote robust dextral looping. Thus, the embryo-scale Nodal L-R asymmetric pathway and organ-intrinsic cellular asymmetries cooperate to indirectly promote dextral heart looping.

2. Materials and methods

2.1. Zebrafish

Princeton University and the University of Oregon Institutional Animal Care and Use Committee (IACUC) husbandry guidelines were adhered to. Embryos were raised at 28 °C and then imaged using a stereomicroscope or processed for *in situ* hybridization. Embryos were staged according to (Kimmel et al., 1995). Lines used were *spaw*^{sa177}, *ntla*^{b160} (Halpern et al., 1993), *spaw*^{t30973} (Noel et al., 2013), Tg

[*myl7:EGFP*]^{twu3} (Huang et al., 2003) and Tg[*-1.0ins:EGFP*] (diIorio et al., 2002). In live embryos, jogging laterality was monitored at 23–25 hpf using a stereomicroscope; heart tubes that deviated from a midline position were deemed to have jogged either to the left or right. Heart looping was scored at 32–36 hpf. If the atrium and ventricle were placed along the central axis of the embryo, we scored the heart as a "middle loop". Otherwise, the two chambers were offset laterally relative to each other, and were scored as either sinistral or dextral loops.

2.2. Wholemount mRNA in situ hybridization

Wholemount mRNA *in situ* hybridization using digoxygenin-labeled probes for *spaw* (Long et al., 2003), *lft1* (Bisgrove et al., 1999), *lft2* (Bisgrove et al., 1999), *ins* (Milewski et al., 1998), *foxa3* (Odenthal and Nusslein-Volhard, 1998), *dand5* (Hashimoto et al., 2004) and *myl7* (Yelon et al., 1999) was performed using standard procedures (Thisse and Thisse, 2014). Embryos were mounted in Canada Balsam (Sigma) with 10% methylsalicylate (Sigma) and visualized using a Leica DMRA microscope and a ProgressC14 Digital Camera (Jenoptik) or a Leica Thunder Model Organism Imager and a DMC4500 Camera (Leica).

2.3. Morpholino oligonucleotide micro-injections

Zebrafish embryos were micro-injected at the 1-cell stage by previously described procedures (Yuan and Sun, 2009). An anti-sense start site *spaw* morpholino oligonucleotide (MO) was injected at 0.5–1 ng/nl. The sequence was 5′-GCACGCTATGACCGGCTGCATTGCG-3' (Long et al., 2003).

2.4. CRISPR

dand5 single guide (gRNAs) were chosen from a previously published look-up table (Wu et al., 2018). Oligos contained a 5' T7 sequence, the nucleotides that target *dand5* and an overlap loop sequence. They were combined with a Bottom Strand Ultramer (see Key Resources Table), annealed and extended to generate full gRNA template, and then RNA was synthesized *in vitro* using a HiScribe T7 High Yield RNA Synthesis kit (NEB, #E2040). Four gRNAs (1000 pg total) were injected along with 1600 pg/nl recombinant Cas9 protein (IDT, #1081058) to generate *dand5* G0 embryos.

2.5. Analysis of CRISPR-induced mutations in G0 embryos

DNA extracted from *dand5* G0 embryos was PCR amplified using primers *dand5_F* and *dand5_R* (see Key Resources Table). PCR product was then cloned using a PCR Cloning Kit (NEB, #E1202), individual colonies were picked, grown in 2 mL cultures and plasmid was then prepped (Qiagen, #27104) and sequenced (Genewiz). Mutations were analyzed by sequence alignments using ApE.

2.6. Statistical analysis

Data visualization and statistical analyses was performed in R (http://www.R-project.org) using the ggplot2 package and the RStudio integrated development environment. Plots for figures were generated using GraphPad Prism version 7.00.

3. Results

To understand how the embryo-scale Nodal/Spaw L-R asymmetric pathway interacts with heart-intrinsic asymmetries, we analyzed heart development in the absence of Spaw signaling. The uncharacterized *spaw*^{sa177} line (Kettleborough et al., 2013) encodes an arginine-to-stop (R275X) nonsense mutation that causes premature truncation of the Spaw protein (Fig. 1B). To determine whether this mutation is a null, we characterized *spaw*^{sa177} mutants and observed a number of L-R abnormalities. First, we analyzed the laterality of heart jogging at 23 hpf by *in situ* hybridization (ISH) for the heart-specific marker *myl7*. While control embryos displayed the expected leftward jogs (J_L), *spaw*^{sa177} mutant hearts jogged either towards the left, right (J_R) or, most commonly, remained midline (J_M) (Fig. 1C). Next, we further assessed organ laterality at later stages by *in situ* hybridization. By 48 hpf, the anlagen of the liver and pancreas are situated to the left and right of the midline, respectively, while the heart has looped dextrally. This arrangement, *situs solitus* (SS), was observed in the majority of control embryos (Fig. 1D). By contrast, *spaw*^{sa177} mutants exhibited defects in organ asymmetry (n = 43/47, 91%) including low levels of reversal of asymmetry, termed *situs inversus* (SI), but mostly discordance between the positioning of different organs, termed heterotaxy (HTX) (Fig. 1D). These L-R defects are consistent with loss of *spaw* function in *spaw*^{sa177} mutants.

To confirm this hypothesis, we assessed Spaw target gene expression. Spaw signaling activates the expression of *lefty1* (*lft1*) in the notochord at the 9 somite stage (ss), with expression continuing throughout somite stages (Burdine and Grimes, 2016; Lenhart et al., 2011), and *lefty2* (*lft2*) in left-sided myocardial cells of the heart cone by the 22 ss (Smith et al., 2008). Both targets were lost in *spaw*^{sa177} mutants (Fig. 1E and F). Since *spaw*^{sa177} mutants were discovered by TILLING, they could harbor unknown mutations that disrupt L-R patterning at the level of KV, upstream of *spaw* expression in the left LPM (Kettleborough et al., 2013; Moens et al., 2008). To exclude this possibility, we assessed *dand5* expression. *dand5* normally surrounds KV, with a R > L bias by the 8–10 ss (Hashimoto et al., 2004), an expression pattern that is invariably altered when upstream asymmetry-generating mechanisms are disrupted (Gourronc et al., 2007; Hojo et al., 2007; Pelliccia et al., 2017). However, R > L *dand5* expression was unaffected in *spaw*^{sa177} mutants (Fig. 1G), suggesting the initial breakage of embryonic L-R symmetry in KV proceeds normally in these mutants. Together, the organ laterality defects and lack of Spaw target gene expression suggest that *spaw*^{sa177} is a loss-of-function allele.

In characterizing *spaw*^{sa177} mutants, we noted subtle differences to previously published *spaw* loss-of-function models (Baker et al., 2008; Montague et al., 2018; Noel et al., 2013). When assessing jogging laterality, we observed mostly J_M heart tubes in *spaw*^{sa177} mutants (Fig. 1C and below), while our previous analysis of morpholino oligonucleotide (MO) knock-down of *spaw* (*MO*^{spaw}) found randomized jogging direction, with J_L, J_M and J_R all equally likely (Lenhart et al., 2013). To extend this comparison, we assessed organ laterality in morphants at 48 hpf. MO knock-down of *spaw* caused distinct defects to the *spaw*^{sa177} mutation, with morphants showing increased *situs* randomization (SS and SI) and reduced HTX compared to mutants (Fig. 1D). This discrepancy could be due to: 1) incomplete knock-down of *spaw* in morphants, 2) *MO*^{spaw} off-target effects, or 3) genetic compensation whereby genetic mutation, but not gene knock-down, changes gene expression at other loci to compensate for the mutation (El-Brolosy and Stainier, 2017; Rossi et al., 2015). To distinguish off-target effects from genetic compensation, we injected *spaw* MO into *spaw*^{sa177} mutants and found that the resulting embryos phenocopied *spaw*^{sa177} mutants but not *MO*^{spaw} (Fig. 1D). This suggests that the *MO*^{spaw} embryo phenotypes are not due to *MO*^{spaw} off-target effects, leaving open the possibility of genetic compensation as a basis for the MO-mutant phenotypic discrepancies. However, we cannot exclude that low-level Spaw signals, beyond the detection limit of *in situ* hybridization, can act to affect heart laterality, as was suggested by Schier and colleagues (Montague et al., 2018). Thus, it could be that low levels of Spaw signal are acting in *MO*^{spaw} embryos but not in *spaw*^{sa177} mutants, and that this contributes to the phenotypic discrepancies.

We next compared *spaw*^{sa177} mutants to the *spaw*^{t30973} allele, which harbors a missense mutation (C401F) towards the C-terminus of the protein (Noel et al., 2013) (Fig. 1A). We observed that a lower proportion of *spaw*^{t30973} mutants exhibited jogging defects than *spaw*^{sa177} mutants (Fig. 1C). Moreover, *trans*-heterozygous *spaw*$^{sa177/t30973}$ embryos displayed intermediate jogging defects (Fig. 1C), suggesting that the

spaw^{t30973} allele is not a complete loss-of-function. Indeed, *spaw*^{t30973} mutants express *spaw* in the LPM at 10 ss (Noel et al., 2013). Since LPM *spaw* is thought to be induced by earlier Spaw signals from around KV, the Spaw^{t30973} protein might possess some residual activity. By contrast, *spaw*^{sa177} mutants never expressed LPM *spaw* when assessed at time points spanning LPM *spaw* initiation in wild-type embryos (Fig. 1H). Additionally, another *spaw* mutant line, generated by CRISPR-Cas9 mutagenesis, was also found to lack LPM *spaw* expression (Montague et al., 2018), further suggesting that *spaw*^{sa177} encodes a null allele.

We next used *spaw*^{sa177} to examine the effect of Spaw on two temporally separated L-R asymmetric events during zebrafish heart morphogenesis: jogging and looping. Using a *myl7:EGFP* transgene that fluorescently labels myocardium in live embryos (Huang et al., 2003), we compared the laterality of jogging and looping in embryos that lack *spaw* expression (*spaw*^{sa177} mutants), express *spaw* on the left (control embryos), or express *spaw* bilaterally (*ntla*^{b160} mutants (Amack and Yost, 2004)) (Fig. 1H). Both *spaw*^{sa177} and *ntla*^{b160} mutants exhibited abnormalities in the direction of jogging and looping. While control embryos demonstrated J_L, >80% of *spaw*^{sa177} and *ntla*^{b160} mutants showed abnormal jogging laterality (Fig. 2A). The majority showed J_M, while a smaller proportion displayed J_R (Fig. 2B). A subset of mutant embryos also displayed J_L. The distribution of jogging directions between *spaw*^{sa177} and *ntla*^{b160} mutants was not different. Interestingly, while lateralized jogs to the left or right were clear in some mutant embryos, jogs were shallower than those observed in control embryos; that is to say that the venous pole of the heart tube, even when clearly lateralized, was closer to the midline in mutant embryos than it was in control embryos.

Compared to the extensive disruption of jogging laterality in mutants, looping laterality was less impacted. Around 50–60% of mutants exhibited normal dextral loops (L_D), while smaller proportions showed either inverted sinistral loops (L_S) or tubes with no obvious directional coiling (L_M) (Fig. 2A and C). Thus, jogging laterality is highly sensitive to Spaw signals whereas looping laterality is less sensitive. Moreover, the same phenotypes result from absence of Spaw asymmetries, whether that arose from loss of *spaw* or bilateral expression of *spaw*. This coheres with the notion that jogging laterality is governed by the embryo-scale L-R Nodal/Spaw pathway while looping laterality depends mostly on heart-intrinsic chirality (Baker et al., 2008; Noel et al., 2013).

Next, we asked whether these two asymmetry-generating mechanisms interacted by assessing whether jogging direction impacts the laterality of subsequent looping. Since we analyzed jogging and looping in the same embryo, we calculated the conditional probability of an embryo attaining a certain laterality of looping given a previous jogging laterality i.e. $P(L_X \mid J_Y)$. This revealed two insights. First, in both *spaw*^{sa177} and *ntla*^{b160} mutants, J_L was predominantly followed by L_D whereas J_R was only followed by L_S in 50–60% of embryos (Fig. 3). Thus, when Spaw-dependent L-R asymmetries are lost, embryos are equally likely to undergo left or right jogs (Fig. 2B), but the likelihood of dextral looping is strongly influenced by the random direction of jogging (Fig. 3). Second, given the condition of a J_M, *spaw*^{sa177} and *ntla*^{b160} mutants exhibited a propensity for normal L_D, which occurred in around 50–60% of embryos, rather than abnormal L_M or L_S (Fig. 3). Thus, heart looping occurs dextrally in most instances even in the absence of asymmetric Spaw signals (Fig. 2A and C) and lateralized jogging (Fig. 3).

As a further test of this idea, we turned to another method of generating embryos with bilateral *spaw* expression. *dand5* is expressed on either side of KV and, as a result of upstream asymmetry-generating mechanisms, becomes repressed on the left side. Since *dand5* is a secreted repressor of Spaw signaling, this promotes left-sided Spaw activation. Thus, in the absence of *dand5*, *spaw* is expressed bilaterally in the LPM (Montague et al., 2018). We generated mosaic mutants called CRISPants by injecting Cas9 enzyme and four *dand5*-targeting gRNAs; such multiplexed targeting promotes high levels of mutagenesis and mutant-like phenotypes in injected G0 embryos (Wu et al., 2018). As expected, these *dand5* G0 embryos exhibited several disruptive mutations at the *dand5* locus (Fig. 4A) and, moreover, demonstrated bilateral expression of *spaw* (n = 48/50; 96%) (Fig. 4B). *dand5* G0 embryos also exhibited laterality defects in heart jogging and looping (Fig. 4C and D). J_M was the most common phenotype, whilst L_D occurred most often, as observed in *spaw*^{sa177} and *ntla*^{b160} mutants (Fig. 4C and D). When we next assessed the relationship between jogging and looping laterality in *dand5* G0 embryos, we again found that the likelihood of dextral looping was strongly influenced by the direction of (randomized) jogging; that is, J_L was almost always followed by L_D, whereas J_R led to a substantial proportion of embryos undergoing L_D or L_M loops (Fig. 4E). Also similar to *spaw*^{sa177} and *ntla*^{b160} mutants, J_M resulted in $L_D >> L_S$ in *dand5* G0 embryos, fitting with the idea that looping laterality is mostly controlled by heart-intrinsic asymmetries (Noel et al., 2013).

Together, these results demonstrate that in the absence of an asymmetric Spaw signal, the likelihood of dextral looping depends on the direction of randomized jogging. We therefore suggest that the role of leftward jogging in zebrafish is to make properly lateralized looping more robust by positioning the heart tube so as to favor dextral looping. The robustness of dextral looping therefore depends on the direction of jogging per se and not on the presence of asymmetric Spaw signals.

Last, we tested for potential consequences of organ L-R defects on zebrafish survivability. As a tool for generating zebrafish with various organ laterality defects, we injected a *spaw* MO into 1-cell zebrafish then sorted the resulting embryos based on the laterality of the heart and pancreas at 2–6 days post fertilization (dpf) into SS, SI or HTX groups. We then raised these fish and assessed their relative viability. Although all three groups showed loss of individuals during embryo-to-adult raising,

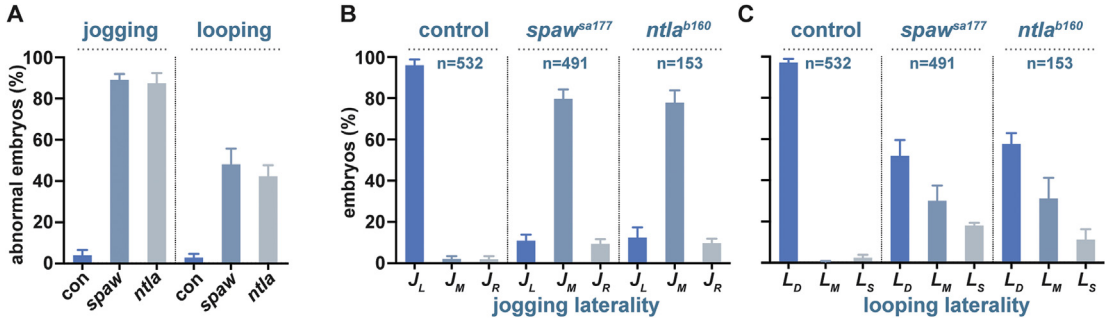

Fig. 2. Jogging and looping laterality in *spaw*^{sa177} and *ntla*^{b160} mutants.
(**A**) Percentage of control (con) and mutant embryos displaying abnormal jogging or looping laterality. (**B–C**) Percentage of embryos showing left (J_L), middle (J_M) or right (J_R) jog (B) and dextral (L_D), middle/no (L_M), or sinistral (L_S) loop (C). *spaw*^{sa177} and *ntla*^{b160} mutants displayed statistically indistinguishable distributions of jogging ($p = 0.80$) and looping ($p = 0.11$) phenotypes; chi-square test applied. In all plots, data represent embryos from at least three clutches. The mean±the standard error of the mean is shown.

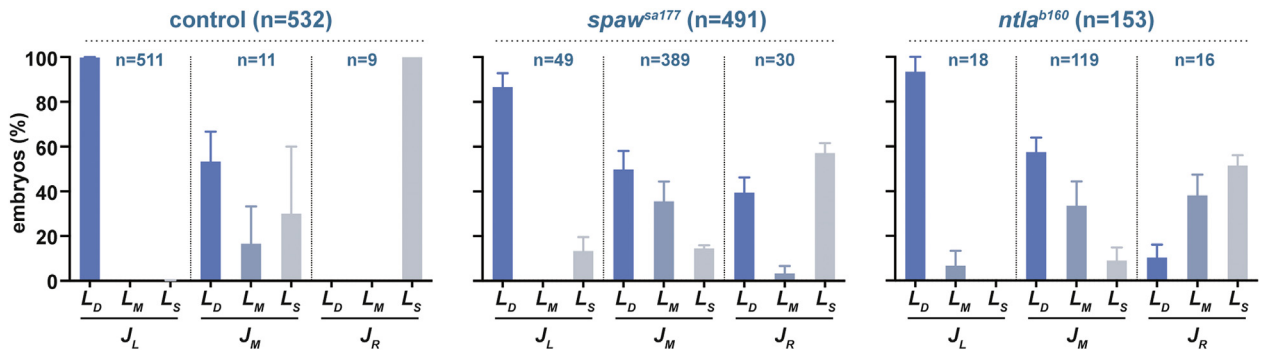

Fig. 3. Relationship between jogging and looping laterality.
Analysis of data from Fig. 2 showing correlation of jogging and looping directions. Bars represent mean of at least three clutches while error bars display the standard error of the mean.

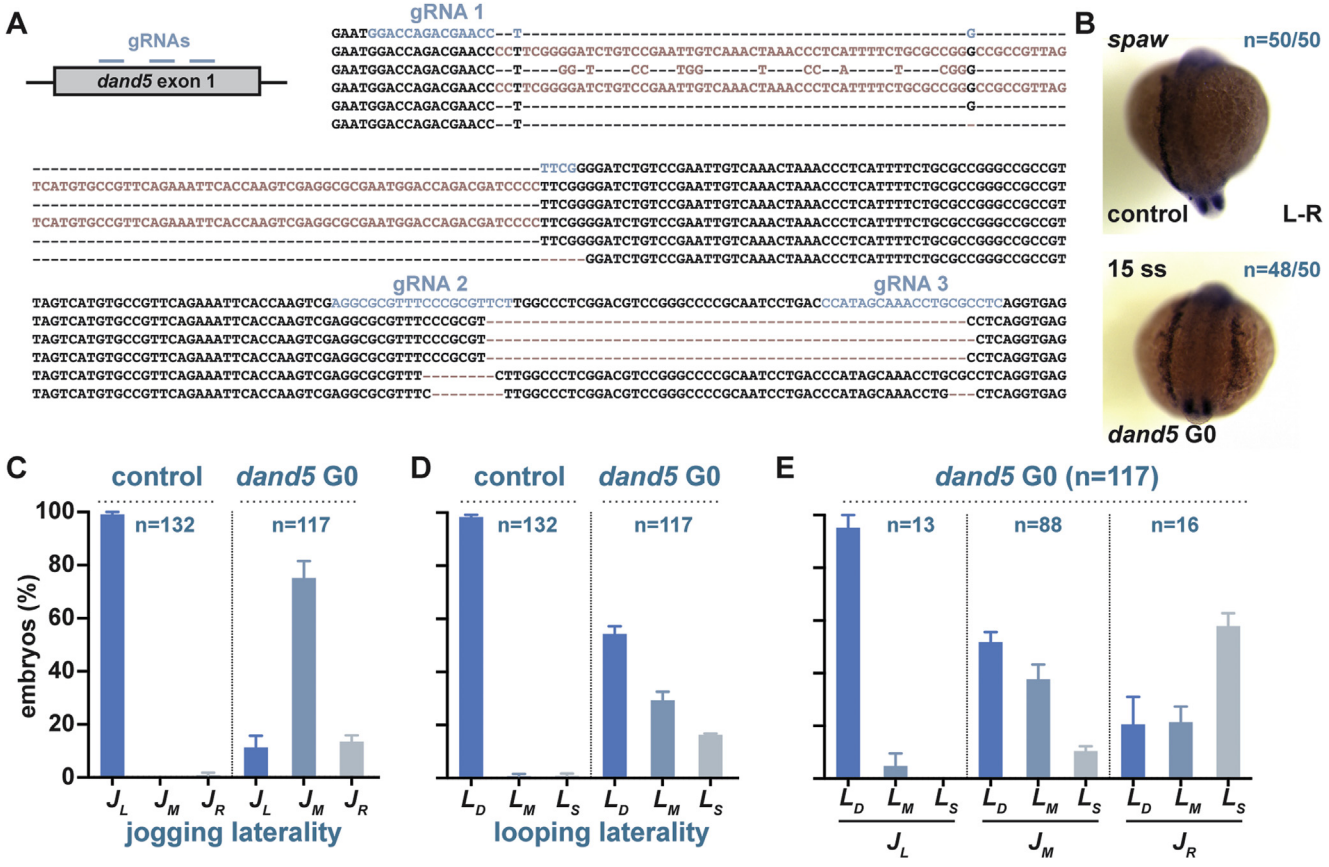

Fig. 4. Relationship between jogging and looping laterality in *dand5* G0 embryos.
(**A**) Schematic of *dand5* exon 1 showing the relative position of three of the four gRNA binding sites used to generate G0 embryos. The fourth was located in a different exon. Sequences show the results from preparing DNA from pools of *dand5* G0 embryos, PCR amplifying a region spanning the three gRNA binding sites, cloning the amplicons, then performing Sanger sequencing of DNA extracted from 5 colonies. None of the sequenced amplicons exhibited wild-type sequence (0%), while 4/5 (80%) showed disruption at multiple gRNA sites and 3/5 (60%) exhibited large deletions between gRNA sites. All amplicons displayed major disruptions, either large insertions and/or deletions or smaller indels at single gRNA sites which shifted the reading frame. (**B**) Representative images of 15-ss embryos stained for *spaw*. Expression was in the left LPM in uninjected embryos and bilateral in 48/50 of *dand5* G0 embryos, the remaining 2/50 exhibited left LPM expression (not shown). (**C-D**) Percentage of embryos showing left (J_L), middle (J_M) or right (J_R) jog (A) and dextral (L_D), middle/no (L_M), or sinistral (L_S) loop (B). (**E**) Relationship between jogging and looping laterality in *dand5* G0 embryos. The experiment was repeated three times and the mean±the standard error of the mean is shown. Scale bar in B represents XX mm.

this was no different to uninjected control animals (Table 1), suggesting that SI and HTX do not impact zebrafish viability in these laboratory conditions. In agreement, intercrosses between *spaw*^{sa177} heterozygotes produced wild-type, heterozygous, and homozygous adult fish at the expected Mendelian frequency (24%, 51%, and 25%, respectively), demonstrating that laterality defects caused by loss of Spaw do not impact zebrafish viability ($p = 0.8$, chi-square test).

4. Discussion

During zebrafish heart morphogenesis, left-sided Spaw signals drive the proper laterality of heart jogging to give rise to a leftward-pointing

Table 1
Percent of zebrafish of different laterality classes that survived to adulthood after being raised in laboratory conditions.

	Situs solitus (SS)	*Situs inversus* (SI)	Heterotaxia (HTX)
Uninjected	60.3% (n = 78)	–	100% (n = 1)
MO^{spaw}	59.4% (n = 101)	83.3% (n = 36)	72.2% (n = 115)

Data represents the sum of three independent trials.

tube (Baker et al., 2008; de Campos-Baptista et al., 2008; Rohr et al., 2008; Smith et al., 2008) whereas dextral looping is driven mostly by heart-intrinsic asymmetries (Noel et al., 2013). However, the role of heart jogging has remained unknown and the interaction between these two asymmetric morphogenetic events is not understood. Here, we analyzed the laterality of heart jogging and looping in live embryos lacking Spaw-derived L-R asymmetries. As expected, we found that loss of Spaw asymmetry impacts jogging laterality and, as such, we consider Spaw to be an Inducer of asymmetry, in line with terminology previously defined (Signore et al., 2016). In the absence of the Inducer, heart tubes cannot attain proper laterality in the majority of cases and when they do, this happens randomly, with the same proportion exhibiting correct laterality as inverted laterality. Intriguingly, both absence of Spaw (*spaw*^{sa177}) and bilateral Spaw (*ntla*^{b160}) led to the same jogging phenotype: mostly middle jogs, but with a minority of embryos attaining an asymmetric jog. *dand5* CRISPant embryos, which also had bilateral *spaw* expression, similarly exhibited mostly middle jogs. The proportion of embryos with asymmetric jogs was similar between *spaw*^{sa177} and *ntla*^{b160} mutants and *dand5* CRISPants while there was no statistically significant bias towards left over right jog or vice versa.

We might explain the small incidence of asymmetric jogging in *ntla*^{b160} mutants by invoking stochastic L-R asymmetries in the level of Spaw. By analogy, the sensory vesicle of ascidians attains morphological asymmetry owing to Nodal-dependent clockwise rotation of the neural tube (Taniguchi and Nishida, 2004). When Nodal is present bilaterally, the vesicle position becomes randomized (Nishide et al., 2012), which is speculated to result from stochastic L-R asymmetries in the strength of Nodal signal (Signore et al., 2016). However, this cannot account for the asymmetric jogs observed in *spaw*^{sa177} mutants. And since randomized jogging occurs at a low level and approximately the same frequency in both *spaw*^{sa177} and *ntla*^{b160} mutants, we suggest that randomized jogging is likely occasionally achieved in both mutants via the same, unknown, mechanism.

The laterality of heart looping in *spaw*^{sa177} and *ntla*^{b160} mutants, and *dand5* CRISPants, was more mildly impacted, coherent with a Spaw-independent mechanism for dextral looping. Indeed, since hearts cultured *ex vivo* undergo dextral looping (Noel et al., 2013), a major driving force of looping laterality must come from a heart-intrinsic source. Nevertheless, we find that 30–40% of *spaw*^{sa177} and *ntla*^{b160} mutants, and *dand5* CRISPants, still loop incorrectly, clearly demonstrating a role for asymmetric Spaw in the consistent generation of a dextrally looped heart. Spaw therefore appears to act as a Modulator of looping (Signore et al., 2016), rather than as an Inducer, increasing the likelihood of a correctly lateralized loop. This interpretation raises the question of how Spaw functions as a laterality Modulator of looping.

By monitoring the same embryo at different developmental time points, we found a correlation between jogging and looping laterality in embryos with symmetrical Spaw activity. Mutants that jogged left almost always looped dextrally. By contrast, mutants that jogged right only looped sinistrally about half the time. This suggests that the heart-intrinsic driver of looping laterality is more effective at generating correctly lateralized loops when the heart tube points to the left of the embryo, even in the absence of Spaw asymmetries. Given this, we suggest that the Modulating role of Spaw in looping is not direct, but instead is a consequence of its earlier role as an Inducer of jogging laterality. Accordingly, jogging itself could be considered a Modulator of looping laterality, since left jogging is sufficient for dextral looping in the absence

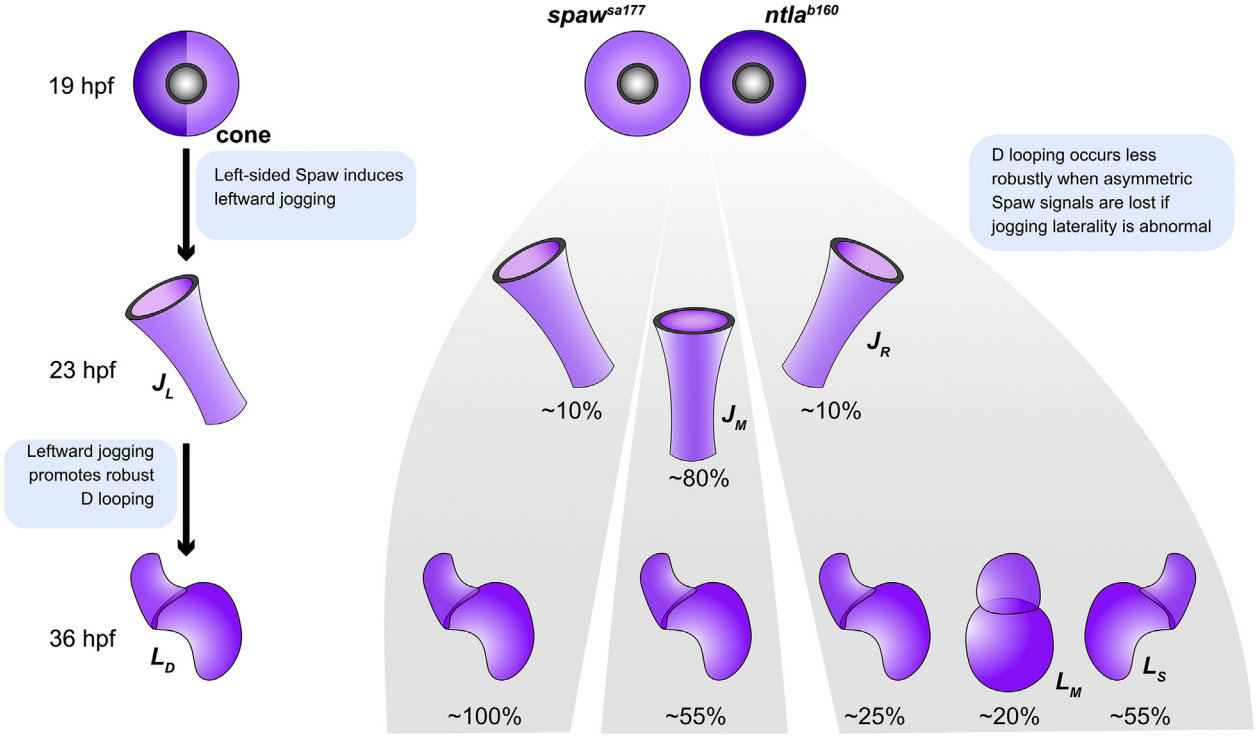

Fig. 5. Left heart jogging increases the robustness of dextral looping.
Left-sided Spaw signals induce left heart jogging which then promotes dextral looping. In mutants with symmetrically-acting Spaw, hearts that happen to jog to the left always loop dextrally whereas hearts that jog to the right show a mixture of looping lateralities. Thus, dextral looping occurs less robustly when asymmetric Spaw signals are lost but only if jogging also occurs improperly. Looping direction therefore controls the robustness of jogging in a Spaw-independent manner. This model suggests the function of left jogging is to increase the robustness of dextral looping.

of Spaw asymmetry. Thus, our data suggest a hitherto unappreciated role for lateralized jogging: to increase the robustness of dextral looping (Fig. 5).

We noted that occasional left or right jogs in the absence of Spaw are 'weak' i.e. the venous pole of the heart tube is leftward but closer to the midline in *spaw*^{sa177} mutants that jog left than in wild-type embryos that jog left. Similarly, right jogs in *spaw*^{sa177} mutants are 'weak', and are not as far to the right as jogs are to the left in controls. Our model would predict that a stronger right-sided jog would be more likely to produce a sinistral loop, and indeed this is the case. Stronger right jogs are observed in mutants of the cilia motility gene *lrrc50* (called *swt*) (Sullivan-Brown et al., 2008), where they arise because *spaw* is often expressed exclusively in the right LPM. In these mutants, right jogs were followed by sinistral loops in 91% of embryos (Baker et al., 2008). This was originally interpreted as demonstrating a role for Nodal signaling in looping laterality, but we suggest that the heart-intrinsic chirality generator is less able to overcome the abnormal jogging phenotype when the displacement of the tube to the right is larger. That is to say that it is the difference in the strength of the right jog in *spaw*^{sa177} and *swt* mutants that results in differences in the amount of dextral looping, and not a direct influence of Nodal signaling on looping laterality.

Last, we observed that zebrafish with aberrant L-R patterning, including heterotaxy, survive comparably to controls in a laboratory setting with ample food and space. In humans, heterotaxy is associated with low viability due in part to congenital heart defects (Desgrange et al., 2018). Mouse embryos with complex L-R defects are often non-viable and typically arrest at embryonic days 13.5–15.5 owing to heart defects (Field et al., 2011; Grimes et al., 2016; Shiratori et al., 2006). In contrast to the four chambered hearts of humans and mice, zebrafish have only two chambers and less complicated connections to the vasculature (Grant et al., 2017). The fact that L-R patterning mutants including *spaw*, *oep*, and *dand5* are viable and fertile shows that altering the L-R asymmetry of the zebrafish heart does not impact survivability. This raises the question of what drives the retention of L-R asymmetry in zebrafish. While we cannot rule out heart asymmetry defects as causing reduced survivability in wild or stressed environments, we speculate that brain asymmetries, which are known to control various aspects of zebrafish behavior including anxiety, fear responses, response to light and feeding behavior (Duboue et al., 2017; Facchin et al., 2015; Zhang et al., 2017), might drive the maintenance of asymmetry. Indeed, behavioral defects resulting from abnormal brain asymmetry might be expected to have less of an impact on survivability in a laboratory setting compared with a wild environment. Asymmetric *spaw* signals control many aspects of brain asymmetry in zebrafish, whereas asymmetric Nodal does not control brain asymmetries in mammals (Gunturkun and Ocklenburg, 2017). This molecular connection between brain and visceral asymmetry in the fish might then contribute to the evolutionary maintenance of consistent body asymmetry, with the need for a properly asymmetric brain resulting in a consistently asymmetric viscera. It will be interesting to test whether zebrafish with different brain asymmetries survive equally well compared with wild-type in environments where food supply and mate competition are competitive.

5. Conclusions

Left-sided Nodal/Spaw signals drive the initial leftward positioning of the linear heart tube. Later, asymmetric looping morphogenesis is governed by heart-intrinsic chirality-generating mechanisms and not embryo-level Nodal/Spaw signals. We find that these two mechanisms interact, and that the positioning of the heart tube initially to the left of the midline increases the robustness of dextral looping morphogenesis.

Author contributions

DTG conceived the project, performed experiments and analyzed data. VLP, GL-A, JS-R and ZHI performed experiments and analyzed data. RDB analyzed data and supervised the project. DTG wrote the manuscript with input from all authors. All authors read and approved the final manuscript.

Acknowledgements

We thank Phillip Johnson, Cori Hasty as well as the University of Oregon Aquatics Facility and Judith Peirce for zebrafish husbandry, Alessandro Giammei for artwork, Jose Pelliccia and Nicholas F. C. Morante for experimental help and Jeroen Bakkers for reagents. DTG acknowledges support of the American Heart Association (16POST31390023), the National Institute of Arthritis and Musculoskeletal and Skin Diseases of the National Institutes of Health (R00AR070905), the University of Oregon, as well as the Developmental Biology Early Career Researcher Program. Work in the Burdine laboratory is supported by the National Institutes of Health. The funding sources had no direct role in this study.

References

Amack, J.D., Yost, H.J., 2004. The T box transcription factor no tail in ciliated cells controls zebrafish left-right asymmetry. Curr. Biol. 14, 685–690.
Baker, K., Holtzman, N.G., Burdine, R.D., 2008. Direct and indirect roles for Nodal signaling in two axis conversions during asymmetric morphogenesis of the zebrafish heart. Proc. Natl. Acad. Sci. U. S. A. 105, 13924–13929.
Bisgrove, B.W., Essner, J.J., Yost, H.J., 1999. Regulation of midline development by antagonism of lefty and nodal signaling. Development 126, 3253–3262.
Bornens, M., 2012. The centrosome in cells and organisms. Science 335, 422–426.
Burdine, R.D., Grimes, D.T., 2016. Antagonistic interactions in the zebrafish midline prior to the emergence of asymmetric gene expression are important for left-right patterning. Philos. Trans. R. Soc. Lond. B Biol. Sci. 371.
Chen, J.N., van Eeden, F.J., Warren, K.S., Chin, A., Nusslein-Volhard, C., Haffter, P., Fishman, M.C., 1997. Left-right pattern of cardiac BMP4 may drive asymmetry of the heart in zebrafish. Development 124, 4373–4382.
Chin, A.J., Tsang, M., Weinberg, E.S., 2000. Heart and gut chiralities are controlled independently from initial heart position in the developing zebrafish. Dev. Biol. 227, 403–421.
de Campos-Baptista, M.I., Holtzman, N.G., Yelon, D., Schier, A.F., 2008. Nodal signaling promotes the speed and directional movement of cardiomyocytes in zebrafish. Dev. Dynam. 237, 3624–3633.
Desgrange, A., Le Garrec, J.F., Meilhac, S.M., 2018. Left-right asymmetry in heart development and disease: forming the right loop. Development 145.
diIorio, P.J., Moss, J.B., Sbrogna, J.L., Karlstrom, R.O., Moss, L.G., 2002. Sonic hedgehog is required early in pancreatic islet development. Dev. Biol. 244, 75–84.
Duboue, E.R., Hong, E., Eldred, K.C., Halpern, M.E., 2017. Left habenular activity attenuates fear responses in larval zebrafish. Curr. Biol. 27, 2154–2162 e2153.
El-Brolosy, M.A., Stainier, D.Y.R., 2017. Genetic compensation: a phenomenon in search of mechanisms. PLoS Genet. 13, e1006780.
Facchin, L., Duboue, E.R., Halpern, M.E., 2015. Disruption of epithalamic left-right asymmetry increases anxiety in zebrafish. J. Neurosci. 35, 15847–15859.
Field, S., Riley, K.L., Grimes, D.T., Hilton, H., Simon, M., Powles-Glover, N., Siggers, P., Bogani, D., Greenfield, A., Norris, D.P., 2011. Pkd1l1 establishes left-right asymmetry and physically interacts with Pkd2. Development 138, 1131–1142.
Gourronc, F., Ahmad, N., Nedza, N., Eggleston, T., Rebagliati, M., 2007. Nodal activity around Kupffer's vesicle depends on the T-box transcription factors Notail and Spadetail and on Notch signaling. Dev. Dynam. 236, 2131–2146.
Grant, M.G., Patterson, V.L., Grimes, D.T., Burdine, R.D., 2017. Modeling syndromic congenital heart defects in zebrafish. Curr. Top. Dev. Biol. 124, 1–40.
Grimes, D.T., 2019. Making and breaking symmetry in development, growth and disease. Development 146.
Grimes, D.T., Burdine, R.D., 2017. Left-right patterning: breaking symmetry to asymmetric morphogenesis. Trends Genet. 33, 616–628.
Grimes, D.T., Keynton, J.L., Buenavista, M.T., Jin, X., Patel, S.H., Kyosuke, S., Vibert, J., Williams, D.J., Hamada, H., Hussain, R., Nauli, S.M., Norris, D.P., 2016. Genetic analysis reveals a hierarchy of interactions between polycystin-encoding genes and genes controlling cilia function during left-right determination. PLoS Genet. 12, e1006070.
Gunturkun, O., Ocklenburg, S., 2017. Ontogenesis of lateralization. Neuron 94, 249–263.
Halpern, M.E., Ho, R.K., Walker, C., Kimmel, C.B., 1993. Induction of muscle pioneers and floor plate is distinguished by the zebrafish no tail mutation. Cell 75, 99–111.
Hashimoto, H., Rebagliati, M., Ahmad, N., Muraoka, O., Kurokawa, T., Hibi, M., Suzuki, T., 2004. The Cerberus/Dan-family protein Charon is a negative regulator of Nodal signaling during left-right patterning in zebrafish. Development 131, 1741–1753.
Hojo, M., Takashima, S., Kobayashi, D., Sumeragi, A., Shimada, A., Tsukahara, T., Yokoi, H., Narita, T., Jindo, T., Kage, T., Kitagawa, T., Kimura, T., Sekimizu, K., Miyake, A., Setiamarga, D., Murakami, R., Tsuda, S., Ooki, S., Kakihara, K., Naruse, K., Takeda, H., 2007. Right-elevated expression of charon is regulated by fluid flow in medaka Kupffer's vesicle. Dev. Growth Differ. 49, 395–405.

Holtzman, N.G., Schoenebeck, J.J., Tsai, H.J., Yelon, D., 2007. Endocardium is necessary for cardiomyocyte movement during heart tube assembly. Development 134, 2379–2386.

Huang, C.J., Tu, C.T., Hsiao, C.D., Hsieh, F.J., Tsai, H.J., 2003. Germ-line transmission of a myocardium-specific GFP transgene reveals critical regulatory elements in the cardiac myosin light chain 2 promoter of zebrafish. Dev. Dynam. 228, 30–40.

Kettleborough, R.N., Busch-Nentwich, E.M., Harvey, S.A., Dooley, C.M., de Bruijn, E., van Eeden, F., Sealy, I., White, R.J., Herd, C., Nijman, I.J., Fenyes, F., Mehroke, S., Scahill, C., Gibbons, R., Wali, N., Carruthers, S., Hall, A., Yen, J., Cuppen, E., Stemple, D.L., 2013. A systematic genome-wide analysis of zebrafish protein-coding gene function. Nature 496, 494–497.

Kimmel, C.B., Ballard, W.W., Kimmel, S.R., Ullmann, B., Schilling, T.F., 1995. Stages of embryonic development of the zebrafish. Dev. Dynam. 203, 253–310.

Lebreton, G., Geminard, C., Lapraz, F., Pyrpassopoulos, S., Cerezo, D., Speder, P., Ostap, E.M., Noselli, S., 2018. Molecular to organismal chirality is induced by the conserved myosin 1D. Science 362, 949–952.

Lenhart, K.F., Holtzman, N.G., Williams, J.R., Burdine, R.D., 2013. Integration of nodal and BMP signals in the heart requires FoxH1 to create left-right differences in cell migration rates that direct cardiac asymmetry. PLoS Genet. 9, e1003109.

Lenhart, K.F., Lin, S.Y., Titus, T.A., Postlethwait, J.H., Burdine, R.D., 2011. Two additional midline barriers function with midline lefty1 expression to maintain asymmetric Nodal signaling during left-right axis specification in zebrafish. Development 138, 4405–4410.

Levin, M., Klar, A.J., Ramsdell, A.F., 2016. Introduction to provocative questions in left-right asymmetry. Philos. Trans. R. Soc. Lond. B Biol. Sci. 371.

Long, S., Ahmad, N., Rebagliati, M., 2003. The zebrafish nodal-related gene southpaw is required for visceral and diencephalic left-right asymmetry. Development 130, 2303–2316.

Milewski, W.M., Duguay, S.J., Chan, S.J., Steiner, D.F., 1998. Conservation of PDX-1 structure, function, and expression in zebrafish. Endocrinology 139, 1440–1449.

Moens, C.B., Donn, T.M., Wolf-Saxon, E.R., Ma, T.P., 2008. Reverse genetics in zebrafish by TILLING. Briefings Funct. Genomics Proteomics 7, 454–459.

Montague, T.G., Gagnon, J.A., Schier, A.F., 2018. Conserved regulation of Nodal-mediated left-right patterning in zebrafish and mouse. Development 145.

Nishide, K., Mugitani, M., Kumano, G., Nishida, H., 2012. Neurula rotation determines left-right asymmetry in ascidian tadpole larvae. Development 139, 1467–1475.

Noel, E.S., Verhoeven, M., Lagendijk, A.K., Tessadori, F., Smith, K., Choorapoikayil, S., den Hertog, J., Bakkers, J., 2013. A Nodal-independent and tissue-intrinsic mechanism controls heart-looping chirality. Nat. Commun. 4, 2754.

Odenthal, J., Nusslein-Volhard, C., 1998. Fork head domain genes in zebrafish. Dev. Gene. Evol. 208, 245–258.

Pelliccia, J.L., Jindal, G.A., Burdine, R.D., 2017. Gdf3 is required for robust Nodal signaling during germ layer formation and left-right patterning. Elife 6.

Ray, P., Chin, A.S., Worley, K.E., Fan, J., Kaur, G., Wu, M., Wan, L.Q., 2018. Intrinsic cellular chirality regulates left-right symmetry breaking during cardiac looping. Proc. Natl. Acad. Sci. U. S. A. 115, E11568–E11577.

Rohr, S., Otten, C., Abdelilah-Seyfried, S., 2008. Asymmetric involution of the myocardial field drives heart tube formation in zebrafish. Circ. Res. 102, e12–19.

Rossi, A., Kontarakis, Z., Gerri, C., Nolte, H., Holper, S., Kruger, M., Stainier, D.Y., 2015. Genetic compensation induced by deleterious mutations but not gene knockdowns. Nature 524, 230–233.

Shiratori, H., Yashiro, K., Shen, M.M., Hamada, H., 2006. Conserved regulation and role of Pitx2 in situs-specific morphogenesis of visceral organs. Development 133, 3015–3025.

Signore, I.A., Palma, K., Concha, M.L., 2016. Nodal signalling and asymmetry of the nervous system. Philos. Trans. R. Soc. Lond. B Biol. Sci. 371.

Smith, K.A., Chocron, S., von der Hardt, S., de Pater, E., Soufan, A., Bussmann, J., Schulte-Merker, S., Hammerschmidt, M., Bakkers, J., 2008. Rotation and asymmetric development of the zebrafish heart requires directed migration of cardiac progenitor cells. Dev. Cell 14, 287–297.

Stainier, D.Y., Lee, R.K., Fishman, M.C., 1993. Cardiovascular development in the zebrafish. I. Myocardial fate map and heart tube formation. Development 119, 31–40.

Sullivan-Brown, J., Schottenfeld, J., Okabe, N., Hostetter, C.L., Serluca, F.C., Thiberge, S.Y., Burdine, R.D., 2008. Zebrafish mutations affecting cilia motility share similar cystic phenotypes and suggest a mechanism of cyst formation that differs from pkd2 morphants. Dev. Biol. 314, 261–275.

Taniguchi, K., Maeda, R., Ando, T., Okumura, T., Nakazawa, N., Hatori, R., Nakamura, M., Hozumi, S., Fujiwara, H., Matsuno, K., 2011. Chirality in planar cell shape contributes to left-right asymmetric epithelial morphogenesis. Science 333, 339–341.

Taniguchi, K., Nishida, H., 2004. Tracing cell fate in brain formation during embryogenesis of the ascidian Halocynthia roretzi. Dev. Growth Differ. 46, 163–180.

Tee, Y.H., Shemesh, T., Thiagarajan, V., Hariadi, R.F., Anderson, K.L., Page, C., Volkmann, N., Hanein, D., Sivaramakrishnan, S., Kozlov, M.M., Bershadsky, A.D., 2015. Cellular chirality arising from the self-organization of the actin cytoskeleton. Nat. Cell Biol. 17, 445–457.

Thisse, B., Thisse, C., 2014. In situ hybridization on whole-mount zebrafish embryos and young larvae. Methods Mol. Biol. 1211, 53–67.

Veerkamp, J., Rudolph, F., Cseresnyes, Z., Priller, F., Otten, C., Renz, M., Schaefer, L., Abdelilah-Seyfried, S., 2013. Unilateral dampening of Bmp activity by nodal generates cardiac left-right asymmetry. Dev. Cell 24, 660–667.

Wan, L.Q., Chin, A.S., Worley, K.E., Ray, P., 2016. Cell chirality: emergence of asymmetry from cell culture. Philos. Trans. R. Soc. Lond. B Biol. Sci. 371.

Wu, R.S., Lam II, Clay, H., Duong, D.N., Deo, R.C., Coughlin, S.R., 2018. A rapid method for directed gene knockout for screening in G0 zebrafish. Dev. Cell 46, 112–125 e114.

Yelon, D., Horne, S.A., Stainier, D.Y., 1999. Restricted expression of cardiac myosin genes reveals regulated aspects of heart tube assembly in zebrafish. Dev. Biol. 214, 23–37.

Yuan, S., Sun, Z., 2009. Microinjection of mRNA and morpholino antisense oligonucleotides in zebrafish embryos. J. Vis. Exp. (27) https://doi.org/10.3791/1113 pii: 1113.

Zhang, B.B., Yao, Y.Y., Zhang, H.F., Kawakami, K., Du, J.L., 2017. Left habenula mediates light-preference behavior in zebrafish via an asymmetrical visual pathway. Neuron 93, 914–928 e914.